Open Veterinary Journal, (2024), Vol. 14(12): 3375-3387
ISSN: 2226-4485 (Print)
ISSN: 2218-6050 (Online)
Research Article
DOI: *10.5455/OVJ.2024.v14.i12.22*

Submitted: 29/09/2024 Accepted: 03/11/2024 Published: 31/12/2024

Evaluation of the anti-diabetic and anti-inflammatory potentials of curcumin nanoparticle in diabetic rat induced by streptozotocin

Barakat Alrashdi[1]*, Hussam Askar[2], Mousa Germoush[1], Maged Fouda[1], Ibrahim Abdel-Farid[1], Diaa Massoud[1], Sarah Alzwain[1], Mohamed H.A. Gadelmawla[3] and Mahmoud Ashry[2]

[1]*Biology Department, College of Science, Jouf University, Sakaka, Saudi Arabia*
[2]*Zoology Department, Faculty of Science, Al-Azhar University, 71524 Assuit, Egypt*
[3]*Histology Department, Faculty of Dentistry, Sinai University, Kantara, Egypt*

ABSTRACT

Background: Natural materials are frequently good options for drug development, regardless of their source. It has been demonstrated that curcumin boosts antioxidant capacity and guards against diabetic disorders.

Aim: The current study aimed to evaluate the possible anti-inflammatory and anti-diabetic effects of curcumin-NPs (Cur-NPs) in streptozotocin-induced diabetic rats.

Methods: Four groups of rats were randomly selected; (1) standard control group, (2) Cur-NPs group was given the regular food of rats along with 5 mg/kg of Cur-NPs daily, (3) Diabetic rats in the STZ group served as the positive control, and (4) Included in the STZ~Cur-NPs group were diabetic rats receiving Cur-NPs (5 mg/kg/day).

Results: After receiving Cur-NPs treatment for 6 weeks, the levels of glucose, tumor necrosis factor alpha TNF-alpha, interlukin1 β (IL1β), interlukin-4, interlukin-6, interlukin-10, MDA, and NO in the diabetic animals were significantly reduced. Simultaneously, the levels of insulin, CAT, GPx, GSH, and SOD were significantly increased, approaching the levels of the corresponding healthy animals. Similarly, insulin secretion increased in the islet β-cells as shown by immunohistochemical analysis, indicating improved glycaemic control and eventual glucose commitment to glycolysis; its processes for scavenging free radicals and acting as an antioxidant may explain this behavior.

Conclusion: As a result, our findings aid in the potential characterization and creation of novel therapeutic agents that prevent diabetes.

Keywords: Immunohistochemical, Curcumin-NPs, Diabetes, STZ, Anti-inflammatory.

Introduction

Diabetes mellitus (DM) is a rapidly expanding illness with a significant risk of death and morbidity (Ali *et al.*, 2024). Hyperglycemia, a chronic metabolic disorder characterized by insufficient or absent insulin, is the hallmark of DM (Huang *et al.*, 2005). Diabetes patients with chronic hyperglycemia experience increased oxidative stress, which throws off the body's redox equilibrium because of an overabundance of reactive oxygen species (ROS) (Prasath and Subramanian 2013). Oxidative stress causes an increase in the oxidation of proteins, lipids, carbohydrates, and DNA. It harms organs and tissue as a result (Yachamaneni and Dhanraj 2017). Those with diabetes who have this syndrome experience both micro- and macrovascular complications (Ibrahim *et al.*, 2023).

There is evidence that DM causes increased oxidative stress in the liver (Tolman *et al.*, 2007). Due to the liver's significant role in controlling glucose metabolism (Levinthal and Tavill 1999), Many disorders impacting glycogen metabolism and liver's lipid are brought on by DM (Sanchez *et al.*, 2000). Many disorders impacting the glycogen metabolism and liver's lipids are brought on by DM (Brownlee 2001). Moreover, it is believed that the harmful effects of hyperglycemia harm pancreatic cells, which are among the most susceptible organs to oxidative stress (Robertson *et al.*, 2004). Insulin gene transcription is inhibited and beta cell death is caused by free radical production mediated by glycation (Donath *et al.*, 1999).

The main clinical sign of diabetes, hyperglycemia, is believed to change circulating lipoproteins, vascular matrix components, and vascular cellular metabolism, all of which can lead to problems with the disease (Seedevi *et al.*, 2020). Hyperglycemia causes protein kinase C activity and increases levels of diacylglycerol in the aorta of diabetic rats and dogs that have been given streptozotocin (STZ) (Chattopadhyay and Bandyopadhyay 2005). In a variety of animal models, STZ has long been the drug of choice for inducing

***Corresponding Author:** Barakat Alrashdi. Biology Department, College of Science, Jouf University, Sakaka, Saudi Arabia.
Email: *bmalrashdi@ju.edu.sa*

type 2 diabetes. This well-established paradigm links insulin resistance to insulin insufficiency. In rats, STZ was demonstrated to result in decreased body weight, increased plasma glucose levels, and 17% mortality following a single intravenous administration (Komolafe *et al.*, 2009).

One of the science and technology research areas with the greatest rate of expansion is nanotechnology. The fact that nanoparticles (NPs) are among the most successful drug delivery techniques with high sustenance, efficacy, and specificity, in living systems is therefore greatly applauded (Jose *et al.*, 2015). When compared to normal capsulated or tablet formulations of any medication, N.P.s as a drug delivery technology offers a number of benefits, such as a greater surface-to-mass ratio, high payload capacity, increased drug stability, prolonged blood circulation, and decreased toxicity (Jiang *et al.*, 2008).

Researchers nowadays are focusing on phytocompounds with pharmacological qualities while creating new medications to treat conditions such as diabetes and cancer (Wojcik *et al.*, 2018) Curcumin (Cur), also known as diferuloylmethane, is a polyphenol-containing chemical molecule. It originates from the rhizomes of the turmeric (Curcuma longa) plant, which is a common spice and food preservative in Asian cooking. Immunity and physiological enhancement are only two of the many health advantages that curcumin, a physiologically active substance, offers (Wanninger *et al.*, 2015). It has received praise from numerous researchers for treating chronic conditions including cancer and type 2 diabetes that involve inflammation, oxidative stress, and internal damage (Wojcik *et al.*, 2018). On the other hand, the compound's pharmacologic and therapeutic potential is limited by its poor bioavailability, which results from decreased absorption in the small intestine with rapid breakdown and faster systemic elimination (Shome *et al.*, 2016). As a result, numerous creative methods have been put forth and developed since then to improve curcumin's bioavailability in the biological system, such as loading the substance as a nanoparticle or conjugate (Grama *et al.*, 2013) There are reports that curcumin cannot be completely absorbed and used *in vivo* when it is in its pure form. Curcumin, nanoparticles, and nanocarriers have shown remarkable anti-diabetic properties, outperforming curcumin as a stand-alone drug, according to a substantial body of research (Hettiarachchi *et al.*, 2021). Consequently, the current study's objectives were to demonstrate the antidiactic effects of Curcumin-NPs (Cur-NPs) against STZ-induced diabetic rats using pro-inflammatory cytokine, anti-oxidative stress, histology, and immunohistochemistry (IHC).

Materials and Methods

Chemicals

Egyptian International Center for Import, Nasr City, Cairo, Egypt, made purchases of citric acid (Sigma C1909), sodium citrate (Sigma C0909), curcumin, and STZ, (Sigma 85882).

Preparation of curcumin nanoparticles

A modified emulsion-diffusion-evaporation method was used to produce curcumin-loaded nanoparticles, as previously documented by Devadasu *et al.*, (2011). In summary, 2.5 ml of ethyl acetate was used to dissolve 7.5 mg of curcumin and 50 mg of poly (lactide -co-glycolide) acid (PLGA), which were then agitated at 1,000 rpm for 30 minutes at room temperature to create a homogenous solution. One of the two stabilizing agents, 50 mg of polyvinyl alcohol (PVA), was dissolved in 5 ml of distilled water. During homogenization, the organic phase containing the active component and PLGA was subsequently added to the stabilizer solution drop by drop. For 5 minutes, homogenization was maintained at 15,000 rpm. Following this, the emulsion was put in 20 ml of water to aid in diffusion, and it was agitated all night to guarantee that the organic solvent evaporated completely. Following the completion of the evaporation stage, the solution containing the nanoparticles was centrifuged at 15,000 × g for 15 minutes to extract the free active component and any unbound stabilizer. After separating the supernatant, the pellet was again mixed with 20 ml of water, and PVA was added to the curcumin nanoparticles.

Predicting bioactivity by in silico physicochemical and pharmacokinetic parameters

Drug-likeness is the outcome of a difficult balancing act between several structural and molecular characteristics. These characteristics, which include bioavailability, dispersion, affinity for proteins, reactivity, and many more, influence how a molecule behaves in a living thing. To identify the substructure's characteristics, which ultimately dictate the compounds' physicochemical attributes, the chemical structure of the produced compounds was integrated into the Swiss ADME web tool (Daina *et al.*, 2017).

Prediction of target–ligand interactions

The Swiss target prediction online tool was utilized for target prediction (Daina *et al.*, 2019).

Molecular docking

Docking investigations were conducted with human glucokinase (PDB code: 1V4S) and the program molecular operation environment (MOE) (version 2015.10) (Bank, 2024) (Human species) sourced from the protein data bank (PDB). With the Merck molecular force field (MMFF94), all minimizations were carried out using MOE until a gradient of 0.01 Kcal/mol/A for the root mean square deviation was reached, at which point partial charges were automatically computed. The London ΔG scoring function calculates the ligand's free energy of binding from a specific posture (Bank, 2021). After refining the improved results using the MMFF94 force field, the London ΔG scoring function was employed to rescore them. The output database's dock file was created using various ligand poses, and it

was sorted using the S function—the final stage score that is not zero (Gadelmawla *et al.*, 2022).

Animals

Male adult Wistar albino rats weighing 170–210 g were used for this investigation. They were bought from the National Research Center's Animal Colony in Cairo, Egypt. For 1 week, in suitable plastic cages, the animals were housed to facilitate their acclimatization. There were always extra standard rodent pellets and tap water (Meladco Company, El-Obour City, Cairo, Egypt) accessible. The pellets contained protein 20.3% (20% casein and 0.3% DL-Methionine), fat 5% (corn oil), fiber 5%, salt mixture 3.7%, and vitamin mixture 1%. For the care and use of experimental animals according to the established institutional rules, all animals received human care (Nomination No. AZHAR 17/2023) from the Faculty of Science at Al-Azhar University in Assuit, Egypt.

Induction of diabetes in rats

To dissolve STZ, a cold sodium citrate-citric acid buffer (20 ml sodium citrate (0.1 M) and 30 ml citric acid (0.1 M) at pH = 4.0) was utilized. After a 16-hour fast, the animals received an intraperitoneal injection of 40 mg/kg. The following day, they were given an oral dose of 2–3 ml of a 10% (w/v) sucrose solution. After that, the animals were fasted for the entire night, and a single drop of blood was drawn by nicking the rats' tail veins with sterile surgical scissors. The blood glucose level was measured immediately using the Gluco Dr SUPER SENSOR AGM-2200 glucometer (Korea). Animals with blood glucose levels of more than 240 mg/dl were classified as diabetic (Sultan *et al.*, 2021).

Study animal groups

Following diabetes induction, rats were randomly assigned to four groups of 10, each consisting of normal and diabetic rats; the first group normal rats were used as the control group and were given 2 ml of distilled water (pH 6.8) orally; second group normal rats were given a daily dose of 5 mg/kg of Cur-NPs (Hassan *et al.*, 2023) and assigned to the Cur-NPs group; third group rats with diabetes were given STZ and were identified as the positive control group; and fourth group Cur-NPs were administered daily to STZ-diabetic rats at a dose of 5 mg/kg, and the animals were labeled as (STZ~ curcumin-NPs).

Blood and tissue sampling

Rats were weighed at the conclusion of the 6-week treatment period, fasted for the entire night, and their blood glucose levels were assessed using GlucoDr utilizing blood samples taken from their tails. Following intramuscular injection of sodium pentobarbital 9.1 mg/kg diluted in sterile 0.9% NaCl, blood specimens were extracted from the retro-orbital plexus using heparinized and sterile glass capillaries. Serum was isolated (from whole blood specimens that had been cool-centrifuged for 10 minutes at 3,000 rpm), divided into aliquots, and kept at −80°C until biochemical measurements were determined. The animals were sacrificed right away after their blood was drawn. For histology and immunohistochemical analysis the pancreas immersed in a 10% formalin-saline buffer.

Biochemical determinations

A sterile surgical scissor was used to remove a blood sample from the lateral tail vein, and the Gluco Dr SUPER SENSOR AGM-2200, a Korean glucometer, was used to measure the results.

Oxidative stress and antioxidant assay

Rat reagent ELISA-kits, acquired from Sunlong Biotech Co., China, were used to assess serum GSH, GPx, NO, MDA, CAT, and SOD levels by ELISA technique (Dynatech Microplate Reader Model MR 5000).

Insulin and pro-inflammatory cytokines

Rat ELISA-kits reagent from SinoGeneClon Biotech Co., China were used to measure the concentrations of insulin, tumor necrosis factor alpha (TNF-α), interlukin-4 (IL-4), interlukin-1 beta (IL-1β), interlukin-10 (IL-10), and interlukin-6 (IL-6) using the ELISA technique (Dynatech Microplate Reader Model MR 5000).

Histopathology

After fixing pancreatic specimens in a 10% formaldehyde solution, the samples were processed to create paraffin cubes. Tissue paraffin wax blocks were sliced into 4-µm-thick slices. The tissue sections were deparaffinized, treated with hematoxylin and eosin stain for histopathological analysis, and examined using light microscopy (Leica Microsystems GmbH, Wetzlar, Germany). To reduce bias, a blinded picture analysis was carried out.

Immunohistochemistry

To investigate the expression of the insulin protein and its location inside pancreatic tissues, we utilized IHC. These treatments included dewaxing, rehydrating, and boiling tissue sections in citrate buffer (pH 6.0) to eliminate antigens. To suppress tissue endogenous peroxidase activity, 3% hydrogen peroxide was administered for 20 minutes. In a humidified chamber, 5% bovine serum albumin was employed as a blocking agent to prevent non-specific antibody binding to tissue proteins. As previously described, four-µm slices of pancreatic tissues were immunostained for 90 minutes using primary antibodies against insulin (CAT # 3014; Cell Signaling Technology, Danvers, MA, USA; 1:100). (Crowe and Yue 2019). Following this, the samples were cleaned and exposed to secondary antibodies tagged with HRP for a duration of 30 minutes. Hematoxylin was employed as a counterstain, and the target proteins were stained with a diaminobenzidine (DAB) kit from ScyTek Laboratories, Inc. in Logan, UT, USA. An imaging system for light microscopes (Meiji Techno Co., Japan; Model MX5200L) was used to take pictures of tissue slices. For every specimen, six non-overlapping fields were photographed. Deconvolution and downstream analysis were carried out for data analysis using the ImageJ Fiji program

(version 1.2; https://imagej.net/Fiji/Downloads; NIH, Bethesda, MD, USA) (Gadelmawla *et al.*, 2022). Area percentages for Insulin immunoreaction were calculated for each group using a × 400 magnification. To reduce bias, an image analysis that was blinded was carried out.

Statistical analysis

As previously mentioned (Steel and Torrie 1981), a one-way ANOVA with a Duncan multiple post hoc test was performed at a significance level of $p \leq 0.05$. Software from the Statistical Analysis System Program was utilized.

Ethics approval

All animals received humane care in compliance with the guidelines of the Animal Care and Use Committee of Faculty of Science, Al-Azhar University, Assuit, Egypt, which ethically approved the proposal with number AZHAR 17/2023.

Results <AQ3>

Pharmacokinetic characteristics, bioactivity prediction, and in silico physicochemical descriptors

The number of heavy atoms, rotatable bonds, H-bond donors, acceptors, and donors; the fraction of carbon bond saturation (Csp3), or the number of hybridized carbons in sp3 relative to the total number of carbons; the solubility (S) parameter LogS (SILICOS-IT); the lipophilicity variable iLOGP predicted using the extra XLOGP3, SILICOS-IT, and WLOGP method; and the molar refractivity for each compound were computed (Table 1).

Using the BOILED-Egg model, gastrointestinal absorption and brain penetration were estimated and concluded. Using the Wildman method, the lipophilicity of ferulic acid is calculated as a partition coefficient (P). Curcumin's polarity was determined using the Crippen approach (WLogP) and the topological polar surface area (tPSA) value. As demonstrated in Figure 1 and (Table 2), this model uses the brain or intestinal estimated permeation technique (BOILED-Egg) to identify chemicals that are projected to passively infiltrate through the brain blood barrier (BBB) and those that are expected to passively be received by the gastrointestinal system, which is located in the white (GIT) (Daina and Zoete 2016; Daina *et al.*, 2017).

From pharmacokinetics results, the compounds were predicted to be highly absorbed in the GIT, and cannot penetrate the BBB. Curcumin demonstrated comparable anticipated actions to CYP1A2, CYP2C19, CYP2C9, and CYP3A4 inhibitors. However, it was anticipated that Compound (16) would inhibit CYP2C9 and CYP3A4. Curcumin was assessed using rule-based techniques developed by Lipinski, Ghose, Veber, Egan, and Mueggue (Table 1) to determine the drug-likeness. From the previous data, Curcumin can be considered promising drug candidates for bioactivity studies with a high Abbott bioavailability score as Curcumin showed zero violations (Lipinski *et al.*, 2001).

Table 1. Predicted physiochemical and lipophilicity descriptors of the synthesized compounds.

Properties	Curcumin
Physiochemical:	
Formula	C21H20O6
Molecular weight	368.38 g/mol
Number of heavy atoms	27
Number of aromatic heavy atoms	12
Fraction Csp3	0.14
Number of rotatable bonds	8
Number of H-bond acceptor	6
Number of H-bond donor	2
Molecular reactivity	102.8
TPSA	93.06 Å2
Solubility LogS (SILICOS-IT)	−4.45
Lipophilicity:	
iLOGP	3.27
XLOGP3	3.2
SILICOS-IT	4.04
WLOGP	3.15
Drug-likeness	
Lipinski	+
Ghose	+
Veber	+
Egan	+
Muegge	+
Bioavailability score	0.55
Pharmacokinetics	
GIT absorption	High
BBB permeant	−
P-gp substrate	−
CYP1A2 inhibitor	−
CYP2C19 inhibitor	−
CYP2C9 inhibitor	+
CUP2D6 inhibitor	−
CYP3A4 inhibitor	+
Log Kp (skin permeation)	−6.28 cm/second

TPSA: topological polar surface area, XLOGP3: Atomistic and knowledge-based technique computed by XLOGP program version 3.2.2; iLOGP: In-house physics-based method, The FILTER-IT program and the Wildman-Crippen method are used to calculate the hybrid fragmental/topological method known as SILICOS-IT. The blood-brain barrier (BBB), the gastrointestinal tract (GIT), CYP2C19 (Cytochrome P450 2C19), CYP1A2 (Cytochrome P450 1A2), CYP2C9 (Cytochrome P450 2C9), CYP3A4 (Cytochrome P450 3A4), and CYP2D6 (Cytochrome P450 2D6).

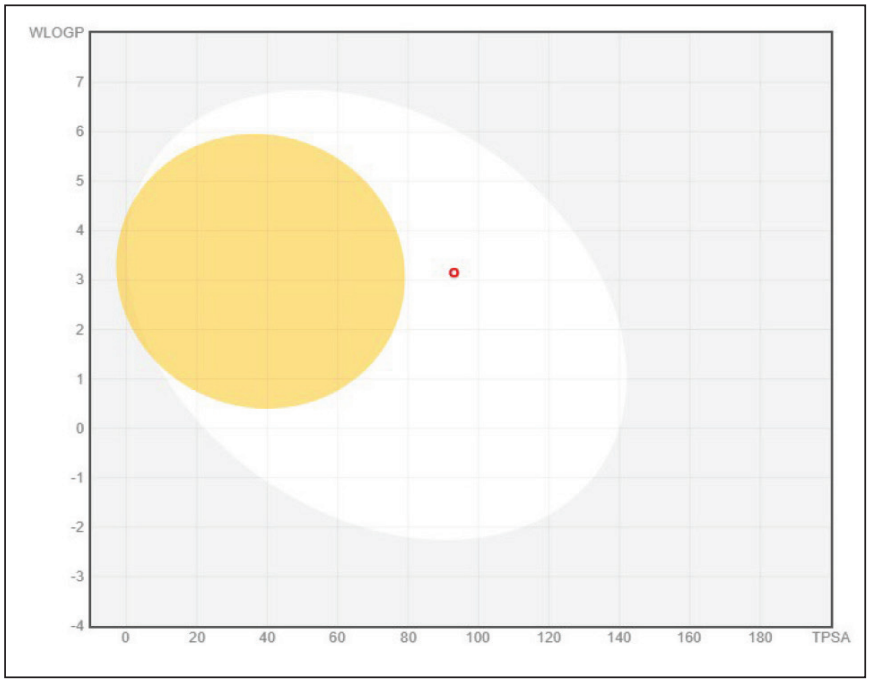

Fig. 1. BOILED-EGG model for Curcumin. The molecules in the white region have the most likelihood of being absorbed by the gastrointestinal tract, while the molecules in the yellow region (yolk) have the highest likelihood of entering the brain. White areas and yolk areas are not antagonistic.

Table 2. The apparent interaction parameters Curcumin with human glucokinase (PDB: 1V4S) (*Homo sapiens*).

Ligand site	Binding site	Type of interaction	Distance of bond (Å)	Binding energy (Kcal/mol)	Total free binding energy (Kcal/mol)
6-ring	Lys 414	Arene-Cation	4.03	−1	
O (8)	Gly 444	Backbone acceptor	2.71	−3.4	
O (9)	Ser 445	Backbone acceptor	3.41	−1.3	−6.395
6-ring	Gly 410	Arene-Hydrogen	3.64	−0.6	
O (18)	Thr 228	Sidechain acceptor	2.97	−1.7	

Lys: Lysine, Gly: Glycine, Ser: Serine, Thy: Threonine.

Target-ligand interaction prediction

The compound's ideal target can be predicted using the Swiss Target Prediction online tool, as seen in Figure 2, that Curcumin may have an enzyme (20%), oxidoreductase (20%), kinase (13.3%), and other receptors (6.7% for each). The prediction of target-ligand interaction gives suggestions of the biological molecules of the cell with which Curcumin could interact. Kinases, oxidoreductase, and enzymes are potential elements in maintaining insulin and islets cells activity.

Molecular docking

GCK is the glucose sensor for the remaining cells in mammals that support glucose homeostasis as well as for controlling the release of insulin by pancreatic β-cells. This includes glucose-sensitive neurons, the adrenal gland, entero-endocrine cells, cells in the anterior pituitary, and other endocrine pancreatic cells (α- and δ-cells) (Matschinsky and Wilson 2019).

In the present study, Curcumin was docked with human glucokinase protein due to their significant correlation to tumor cells. They have been employed in recent docking studies to assess other compounds' antitumor activity (Abbas *et al.*, 2024). As a result, GCK has been singled out in efforts to find a DM cure. Lu *et. al.* (2016) showed that the STZ-induced diabetic murine model exhibits low GCK expression with high blood glucose levels (Lu *et al.*, 2016).

The acquired data of substances firmly demonstrated the binding of targeted ligand sites, Curcumin

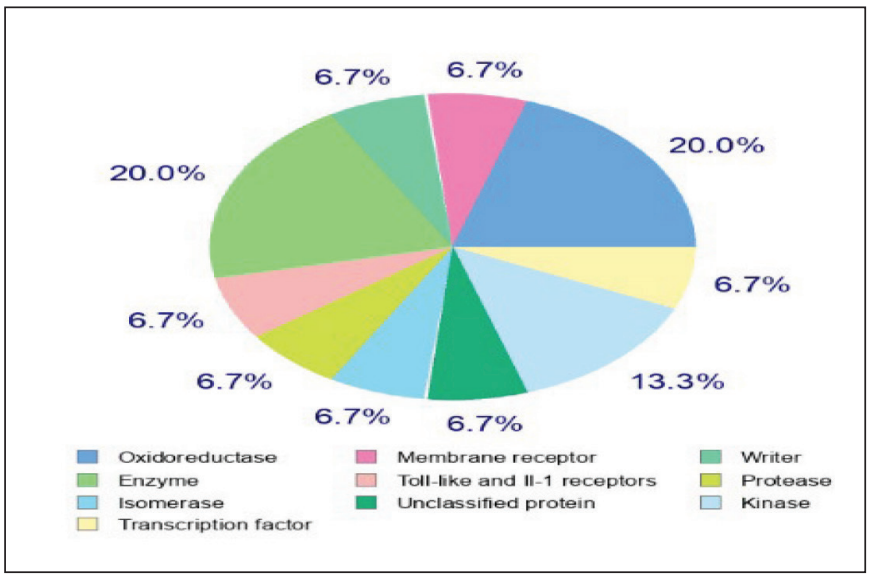

Fig. 2. Swiss Target Prediction Webtool for target prediction of curcumin.

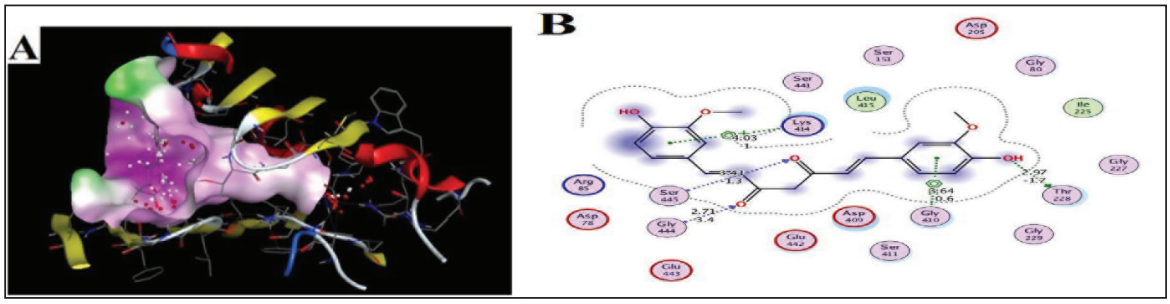

Fig. 3. Docking of human glucokinase (PDB: 1V4S), (A): 3D interaction figure with Curcumin, (B): 2D interaction diagram with Curcumrein.

demonstrated five interactions between the target protein and the target ligand sites, which are 6-ring, Oxygen (O) 8 and 9, 6-ring, and Oxygen (N) 18, via the amino acids Lysine (Lys) 414, Glycine (Gly) 444, Serine (Ser) 445, Glycine (Gly) 410, and Threonine (Thr) 228. The types of interaction bonds clearly appeared as potential interactions with strong peptide bonds (backbone), hydrogen bonds (sidechain), and hydrophobic interactions (Arene-H bonds). The poses form that gave the largest binding energy (−6.395 kcal/mol) was represented in Figure 3A, B and Table 2.

Effect of Cur-NPs on glucose and insulin

When comparing the STZ-induced diabetic group to the control group, the *in vivo* data showed a large rise in blood glucose and a significant decrease in insulin level. Cur-NPs treatment in diabetic rats was found to dramatically boost insulin and decrease glucose levels in comparison to diabetic rats, hence improving insulin and glucose levels towards normal values; data (Table 3).

Effect of Cur-NPs on pro-inflammatory cytokines

The data obtained indicated a significant increase in the levels of TNF-α, IL1β, IL-4, IL-6, and IL-10 in the group with diabetes when compared to the control group. Cur-NPs were administered to STZ rats, and it was observed that all inflammatory cytokines were improved within normal ranges. Specifically, TNF-α, IL1β, IL-4, IL-6, and IL-10 were dramatically reduced in comparison to STZ animals (Fig. 4a–e).

Effect of Cur-NPs on oxidant-antioxidant markers

With respect to Table 4. The serum oxidative stress status significantly worsened after STZ intoxication, as seen by a dramatic decline in GSH levels, CAT, SOD, and GPx activity, as well as a marked increase in blood MDA and NO levels. Cur-NPs treatment of STZ-intoxicated rats resulted in a beneficial change in serum MDA and NO levels as well as a notable increase in GSH, CAT, SOD, and GPx activities compared to the STZ-intoxicated group.

Table 3. Normal, diabetic, and diabetic-treated rats' mean glucose and insulin levels.

	Control	Cur-NPs	STZ	STZ ~ Cur-NPs
Glucose (mg/dl)	88.5 ± 2.6	87.8 ± 2.4	363 ± 13.5*	122 ± 5.3#
Insulin (ng/ml)	2.41 ± 0.77	2.51 ± 0.85	0.66 ± 0.32*	2.31 ± 0.74#

After undergoing a one-way ANOVA and a post hoc test (Duncan) at $p \leq 0.05$, the data are displayed as mean ±standard error. (*) clearly differs from the control group, and (#) considerably differs from the STZ group. (Cur-NPs) curcumin Nanoparticle; (STZ) Streptozotocin.

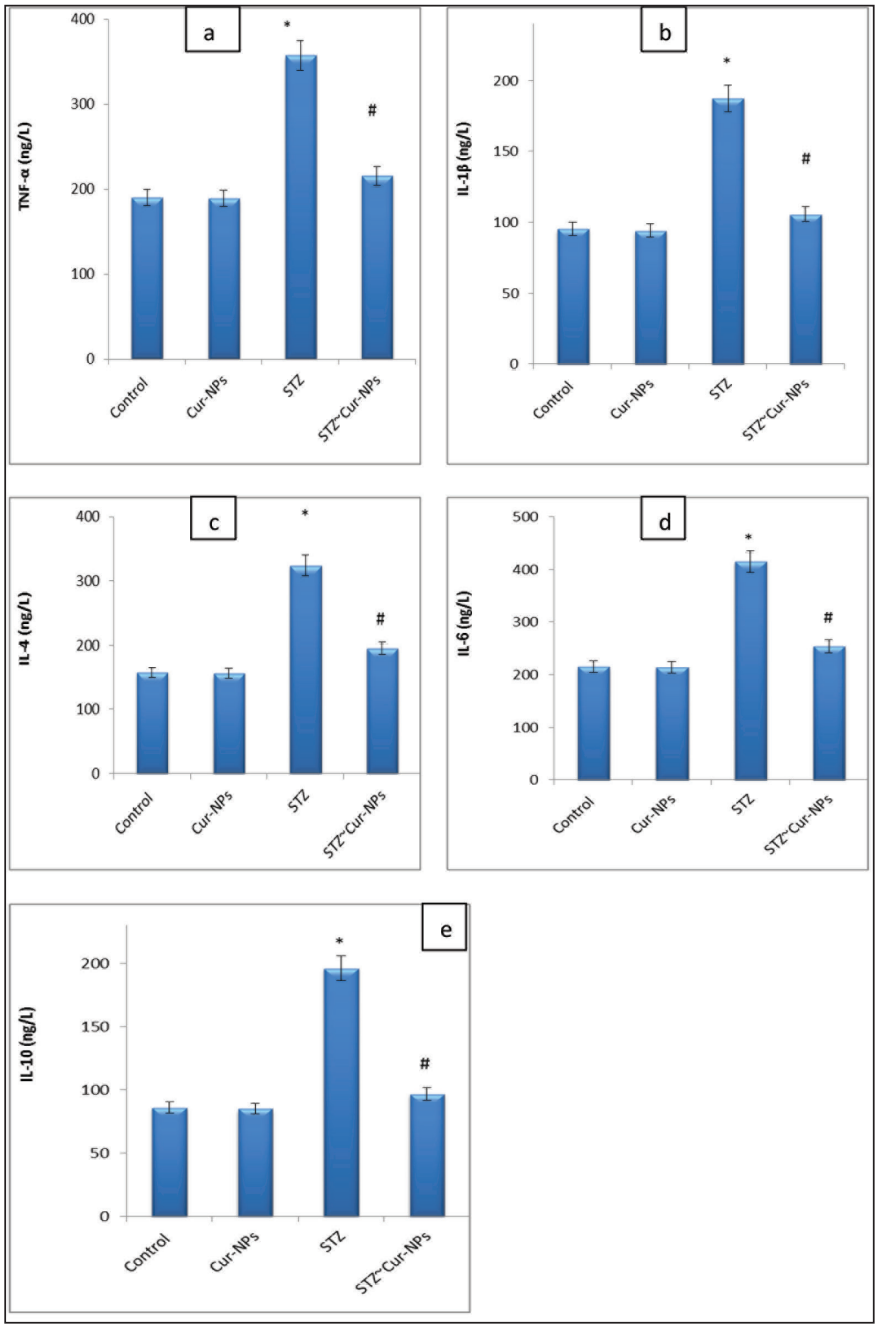

Fig. 4a–e. Serum levels of TNF-α, IL1β, IL-4, IL-6, and IL-10 in male albino rats treated with curcumin NPs, STZ-intoxicated rats, and control rats. (*) clearly differs from the control group, and (#) considerably differs from the STZ group. (Cur-NPs) curcumin Nanoparticle; (STZ) Streptozotocin.

Table 4. Effect of STZ and Cur-NPs on serum MDA, NO, SOD, GPx, GSH and CAT.

	STZ	Cur-NPs	Control	STZ ~ Cur-NPs
MDA (pg/ml)	336.4 ± 10.5*	95.7 ± 6.3	96.8 ± 5.6	115 ± 6.4#
NO (µmol/l)	66.9 ± 7.3*	31.9 ± 3.8	32.6 ± 2.45	44.3 ± 4.2#
GSH (ng/ml)	24.2 ± 4.4*	54.4 ± 4.1	52.3 ± 4.5	46.6 ± 5.2#
SOD (U/l)	19.5 ± 4.6*	46.8 ± 6.4	45.5 ± 3.55	38.7 ± 4.5#
GPx (U/l)	154 ± 5.3*	392 ± 14.6	389 ± 15.4	328 ± 12.7#
CAT (U/l)	11.5 ± 1.14*	29.2 ± 2.77	28.4 ± 1.88	24.5 ± 2.52#

After undergoing a one-way ANOVA and a post hoc test (Duncan) at $p \leq 0.05$, the data are displayed as mean ±standard error. (*) clearly differs from the control group, and (#) considerably differs from the STZ group. (Cur-NPs) curcumin Nanoparticle; (STZ) Streptozotocin.

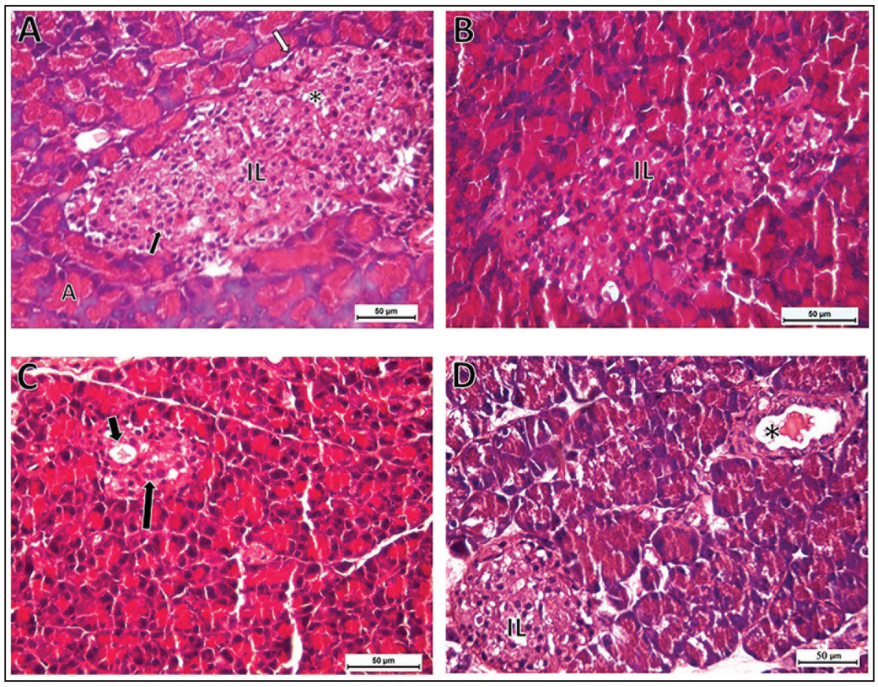

Fig. 5. Photomicrographs of sections in the pancreas of rats (Hand E, X400). (A) Control group showing normal exocrine acini (A), normal islet of Langerhans (IL) consisted of endocrine cellular cords separated by blood capillaries (*), with α-cell (white arrow) with dark oval nucleus located in the periphery, β-cell (black arrow) with oval light nucleus located in the central region. (B) Cur-NPs group revealed normal pancreatic tissue structure. (C) STZ-induced DM showing atrophied islet of Langerhans with prominent space (short arrow) and faint karyolitic cells (long arrow). (D) STZ group treated with Cur-NPs exhibited remarkable improvement with normal islet of Langerhans and congested pancreatic duct (*).

Histopathological examination

The endocrine and exocrine sections of the pancreas were shown to have a normal structure in the control and Cur-NPs groups (Fig. 5A, B). Very few acinar cells had darkly condensed nuclei, and only a tiny number of islets cells in the STZ group sections displayed vacuolations and small darkly pigmented condensed nuclei (Fig. 5C). With the exception of a very small number of darkly stained condensed nuclei in the islets of Langerhans, the pancreas structure (endocrine and exocrine portions) of the STZ group treated with Cur-NPs was almost identical to that of the control group (Fig. 5D).

Immunohistochemistry

The IHC data revealed marked immunostaining of Insulin in both control and Cur-NPs groups. STZ triggered a significant decrease ($p < 0.0001$) in pancreatic protein expression of activated insulin (Fig. 6C). Co-administration of Cur-NPs to STZ-induced DM in rats triggered a significant increase in Insulin ($p = 0.011$).

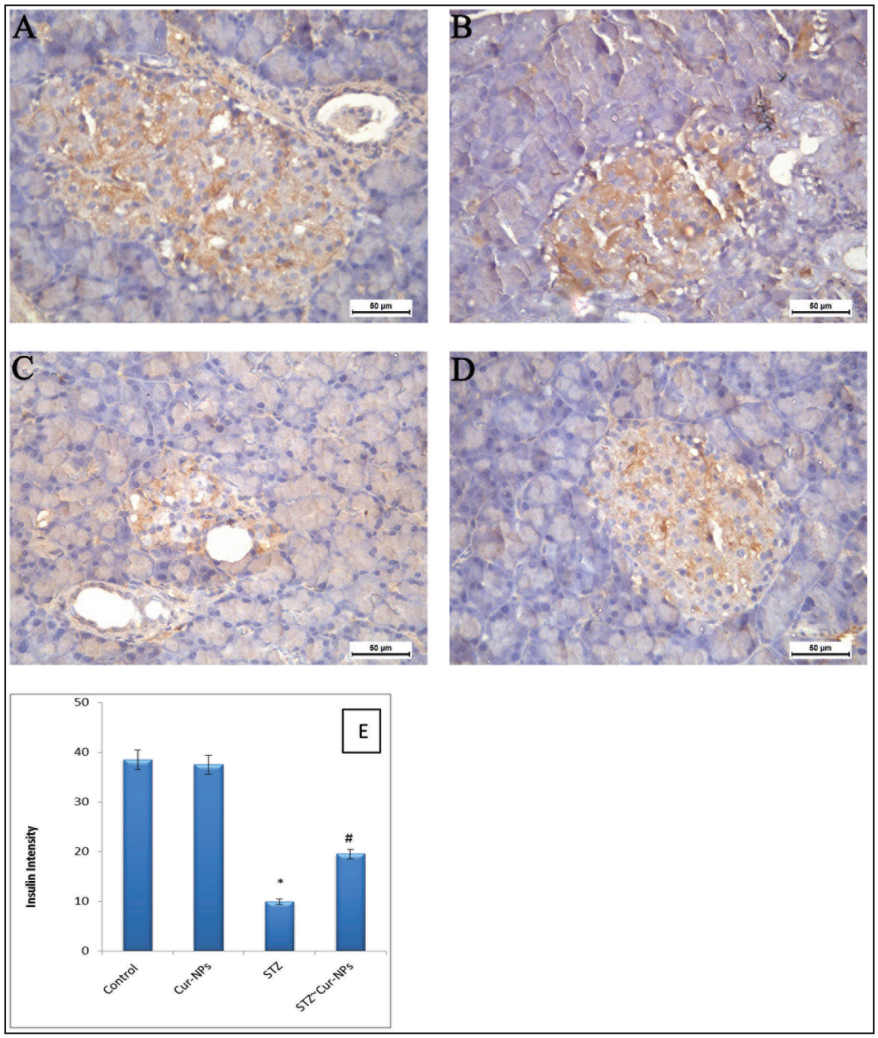

Fig. 6. Ameliorative effect of Cur-NPs on pancreatic protein expression of activated insulin in STZ-induced DM in rats. For $n = 6$ tissues, the photomicrographs are representative. (A–D) Pancreatic tissue photomicrographs from every experimental group. Here, DAB chromogen was used to generate a brown color that represented the immunoreactivity of insulin in the tissues (50-µm scale bar, X400). (E) Insulin expression in pancreatic tissues quantified. Data is shown as mean ± SEM for $n = 6$. * $p < 0.05$ indicated significance when compared to the control group. Compared to STZ group: significance was described by # $p < 0.05$ (as established by the one-way ANOVA and Bonferroni's test).

Discussion

After cancer and cardiovascular diseases, DM ranked third among the country's main causes of death in 2019, according to CDC mortality data. Numerous researchers have proposed various approaches for the management and control of this lifestyle-related illness (Hassan *et al.*, 2023). But despite advances in science and technology, the illness remains uncontrollable. In STZ-induced diabetic rats, the current study aimed to evaluate the anti-inflammatory and anti-diabetic effects of Cur-NPs. Animals used in this investigation were given intraperitoneal injections of 40 mg/kg; those whose blood glucose levels were higher than 240 mg/dl were classified as diabetic. When compared to normal control rats, significantly higher blood glucose and lower insulin levels were seen in the STZ-induced diabetic rats. The results of these investigations align with the latest research (Ali *et al.*, 2024). STZ has been shown to invade insulin-producing β-cells in the pancreas, inducing DM within a week of injection in experimental animal models, as demonstrated by hyperglycemia and hypoinsulinemia (Han *et al.*, 2017). The majority of researchers clarify that the main agents responsible for the *in vivo* pathophysiology of STZ-induced DM are the ROS that STZ triggers (Han *et al.*,

2017). Furthermore, in diabetic circumstances, the elevated glucose level is auto-oxidized, exacerbating the *in vivo* redox balance (Nna *et al.*, 2020). Our findings demonstrated that administering Cur-NPs to diabetic rats improved insulin and glucose levels toward normal values by dramatically raising insulin and lowering glucose levels in comparison to diabetic rats. In addition to its anticancer potential, curcumin has been shown to possess a wide range of other pharmacological and therapeutic qualities, such as antidiabetic, antioxidant, anti-inflammatory, anti-allergies, and anti-lipedema effects (Zhang *et al.*, 2013). Curcumin is an excellent option for treating diabetes because of its advantageous properties. Additionally, it has been reported that following a 9-month curcumin treatment, a sizable cohort of pre-diabetic individuals who were expected to develop type 2 diabetes demonstrated a notable increase in pancreatic beta-cell activity and related glycemic indexes.

Cur-NPs have been used in this investigation to overcome the aforementioned *in vivo* limitations of curcumin. Cur-NPs have been shown in numerous studies to have superior anti-glycemic and insulin sensitivity-enhancing properties (Hassan *et al.*, 2023). Thus, in the current study, the administration of Cur-NPs shows great anti-diabetic potential. Additionally, by reducing lipid peroxidation and suppressing oxidative stress, the combination restores the structures and functions of cells.

It is well known that pancreatic islet cells express the lowest levels of antioxidant enzymes, including superoxide dismutase, glutathione peroxidase, and catalase, as compared to other tissues including the liver, kidney, and adipose tissue (Tiedge *et al.*, 1999). By consuming antioxidant defense components, an increase in free radicals may cause oxidative damage to membranes and the breakdown of cellular activities (Baynes 1991). System of physiological antioxidant defense as supported by SOD, GSH, and CAT. Our findings demonstrated that the administration of Cur-NPs to diabetic rats after their post-treatment resulted in a large recharging of their GSH battery and an increase in the activities of SOD and CAT. Furthermore, Cur-NPs were able to reduce the rise of NO levels compared to the equivalent values of diabetic rats. These outcomes align with earlier research (Hassan *et al.*, 2023).

The intriguing finding, which is consistent with previous findings, suggests that the creation of free radicals triggered by diabetes may have caused peroxidative damage to the liver tissue, which may have further led to the formation of an excessive amount of MDA (Kapoor *et al.*, 2009). Lipid peroxidation produces MDA, an aldehydic byproduct that readily interacts with biomolecules to cause cellular disruption, including β-pancreatic cell disruption, which in turn disrupts glucose metabolism (Belce *et al.*, 2000).

Hyperglycemia in diabetes causes the body to produce free radicals, which impair defense mechanisms and cause cellular processes to be disrupted, membranes to be oxidatively damaged, and lipid peroxidation to be more susceptible (Prasad *et al.*, 2000). Severe hyperglycemia has been linked to increased SOD activity (Greene and Chen, 1999). Important enzymatic antioxidants like SOD and GSH play a role in cellular defense systems and may be helpful in reducing lipid peroxidation, which protects tissues from oxidative damage (Li *et al.*, 2010). Antioxidants are thought to repair damaged extracellular matrix proteins and promote cell development in hyperglycemic environments (Prasad *et al.*, 2000). Furthermore, elevated MDA content in hyperglycemic rats has been documented in the past.

TNF-α, IL-1β, IL-4, IL-6, and IL-10 levels were considerably higher in the current study after STZ treatment than in the control group. These results are consistent with those found in other earlier research (Almasoudi *et al.*, 2024). In diabetic animals under stress, inflammatory cytokines are essential for both antibody release and the inflammatory response (Inoguchi *et al.*, 2003). TNF-α is a strong inflammatory cytokine that is produced by T lymphocytes and macrophages. It has significant effects on DM as it contributes to the development of insulin resistance as well as the advancement of microvascular problems (Dokumacioglu *et al.*, 2018). It has been noted that the primary promoter of tissue and systemic inflammation in DM is IL-4, IL-6, IL-1β, and IL-10, which are important factors in a variety of auto-inflammatory disorders (Borra *et al.*, 2014). Due to their release from adipokines, IL-4, IL-6, IL-1β, and IL-10 are thought to be important in the development of cardiovascular complications of DM, particularly diabetic vasculopathy, as they can affect distant organs such as the heart or vessels through increased vascular and systemic inflammation (Peiro *et al.*, 2017). Additionally, the Cur-NPs reduce lipid peroxidation and inhibit oxidative stress, which helps to restore the structures and activities of cells. As a result, it can also restore the histology and functioning of the pancreatic islets, potentially increasing insulin sensitivity and activity (Thota *et al.*, 2018). As demonstrated by the reduction of pro-inflammatory cytokines and interleukins TNF-a, IL-1β, IL-4, IL-6, and IL-10, it is also known that the antioxidant properties of both adjuvants (curcumin and NPs) can stop the inflammatory aggression of the free radicals (Roxo *et al.*, 2019). Additionally, curcumin has been shown to reduce inflammation and cause the injured pancreatic beta cells to undergo apoptosis, which enhances function and maintains glucose homeostasis (Ganugula *et al.*, 2017).

The study's histological analysis, which demonstrated that STZ caused pancreatic harm in the STZ-treated rats, is consistent with Almasoudi *et al.* (2024). It was also seen that the β-cells were degenerating at different degrees, causing deformation in the architecture of the tissue and passing through small fibrosepta. Diabetes

mellitus results from STZ's selective destruction of pancreatic islet cells that secrete insulin, leaving the cells less active (Tahara *et al.*, 2008). Insulin insufficiency linked to insulin resistance characterizes this well-established paradigm (Abdollahi *et al.*, 2010). When compared to the STZ group, the pancreatic tissues treated with Cur-NPs showed improvement and just minor harm. The proven antioxidant and anti-inflammatory qualities of curcumin help repair pancreatic β-cells and improve diabetic patients' overall metabolism (Wojcik *et al.*, 2018). The bioactive chemical has been shown to block intracellular transcription factors such as NF-κB, activator protein 1, nitric oxide synthase, cyclooxygenase II (COX-2), MMP-9, and STAT3, hence promoting programmed cell death (Ebaid *et al.*, 2021). It is known that inflammation caused by ROS and redox imbalance contribute to the pathogenesis of DM. According to the current study, Cur-NPs regulate the target organs' redox status—the liver and pancreas—by boosting the activity of antioxidant enzymes and proteins that reduce inflammation and the body's toxic burden (Ebaid *et al.*, 2021). It enhances the liver's (improved glucose absorption and glycogen synthesis) and pancreatic's (insulin production and section) functions.

Conclusion

In conclusion, STZ was able to successfully cause hyperglycemia. When STZ was administered, blood glucose (hyperglycemia) increased, and insulin synthesis was lowered. STZ produced more ROS, which led to oxidative stress and anomalies in the metabolism of glucose, favoring hyperglycemia. By triggering the insulin signaling pathway, Cur-NPs reduced the negative effects of STZ and enhanced oxidative damage-induced anomalies of glucose metabolism, such as elevated insulin secretion and decreased blood glucose. It can be inferred that Cur-NPs mitigated oxidative stress damage, hence providing protection against hyperglycemia caused by STZ.

Acknowledgment

The authors extend their appreciation to the Deanship of Scientific Research at Jouf University, Saudi Arabia, for funding this work through research grant number (DSR2022-RG-0117).

Conflict of interest

The authors declare that there is no conflict of interest.

Funding

This work was funded by the Deanship of Scientific Research at Jouf University under Grant Number (DSR2022-RG-0117).

Authors' contributions

B. Alrashdi: Resources, Data curation, Funding acquisition, Project administration, writing-review, and editing. H. Askar: Data curation, Formal analysis, Writing-review, and editing M. Germoush: Data curation, Formal analysis. M. Fouda: Formal analysis, writing original draft. I. Abdel-Farid: Formal analysis, Writing-review, and editing. D. Massoud: Data curation, Formal analysis, Writing-review, and editing. S. Alzwain: Data curation, Formal analysis. M. Gadelmawla: Data curation, Formal analysis, writing original draft. M. Ashry: Conceptualization, Data curation, Formal analysis, Supervision, Writing-review and editing. All authors have read and agreed to the published version of the manuscript.

Data availability

All data generated or analyzed during this study are included in this article.

References

Abbas, A.M., Nasrallah, H.H., Aboelmagd, A., Kishk, S.M., Boyd, W.C., Kalil, H. and Orabi, A.S. 2024. Design, synthesis, anti-inflammatory activity, DFT modeling and docking study of new ibuprofen derivatives. Int. J. Mol. Sci. 25(6), 3558.

Abdollahi, M., Zuki, A., Goh, Y., Rezaeizadeh, A. and Noordin, M. 2010. The effects of *Momordica charantia* on the liver in streptozotocin-induced diabetes in neonatal rats. Afr. J. Biotechnol. 9(31), 5004–5012.

Ali, E.Y., Abu-Elsaoud, A., Moghzi, M.M. and Marie, O.M. 2024. Ethanolic extract of orange leaves ameliorates dyslipidemia in streptozotocin-induced diabetic rats. AELS. 5, 35–41.

Almasoudi, H.H., Nahari, M.H., Binshaya, A.S., Hakami, M.A., Alhazmi, A.Y., Al Shmrany, H., Alqasem, A. and Khanm F.R. 2024. Sakuranetin ameliorates streptozotocin-induced diabetes in rodents by inhibiting caspase-3 activity, modulating hematological parameters, and suppressing inflammatory cytokines: a molecular docking and dynamics study. J. Biomol. Struct. Dyn. 2024, 1–18.

Baynes, J.W. 1991. Role of oxidative stress in development of complications in diabetes. Diabetes 40, 405–412.

Bank. 2024. Bank RPD. RCSB PDB - 1V4S. Crystal structure of human glucokinase [Internet]. Available via https://www.rcsb.org/ structure/1v4s.

Bank. 2021. Bank RPD. RCSB PDB—6MXZ. Structure of 53BP1 Tudor domains in complex with small molecule UNC3474 [Internet]. Available via https://www.rcsb.org/structure/6MXZ.

Belce, A., Uslu, E., Kucur, M., Umut, M., Ipbuker, A. and Seymen, H.O. 2000. Evaluation of salivary sialic acid level and Cu-Zn superoxide dismutase activity in type 1 diabetes mellitus. Tohoku. J. Exp. Med. 192, 219–225.

Borra, S.K., Mahendra, J., Gurumurthy, P., Jayamathi, Iqbal, S.S. and Mahendra, L. 2014. Effect of curcumin against oxidation of biomolecules by hydroxyl radicals. J. Clin. Diagn. Res. 8, CC01–5.

Brownlee, M. 2001. Biochemistry and molecular cell biology of diabetic complications. Nature 414, 813–820.

Chattopadhyay, R. and Bandyopadhyay, M. 2005. Effect of *Azadirachta indica* leaf extract on serum lipid profile changes in normal and streptozotocin induced diabetic rats. Afr. J. Biomed. Res. 8, 101–104.

Crowe, A.R. and Yue, W. 2019. Semi-quantitative determination of protein expression using immunohistochemistry staining and analysis: an integrated protocol. Bio. Protoc. 9(24), e3465.

Daina, A. and Zoete, V. 2016. A BOILED-Egg to predict gastrointestinal absorption and brain penetration of small molecules. Chem. Med. Chem. 11, 1117–11121.

Daina, A., Michielin, O. and Zoete, V. 2017. SwissADME: a free web tool to evaluate pharmacokinetics, drug-likeness and medicinal chemistry friendliness of small molecules. Sci. Rep. 7, 42717.

Daina, A., Michielin, O. and Zoete, V. 2019. SwissTargetPrediction: updated data and new features for efficient prediction of protein targets of small molecules. Nucleic Acids Res. 47, 357–364.

Devadasu VR, Wadsworth RM and Ravi Kumar MNV (2011). Protective effects of nanoparticulate coenzyme Q10 and curcumin on inflammatory markers and lipid Metabolism in streptozotocin-induced diabetic rats: A possible remedy to diabetic complications. Drug Deliv Transl Res., 1: 448–455.

Dokumacioglu, E., Iskender, H., Sen, T.M., Ince, I., Dokumacioglu, A., Kanbay, Y., Erbas, E. and Saral, S. 2018. The effects of hesperidin and quercetin on serum tumor necrosis factor-alpha and interleukin-6 levels in streptozotocin-induced diabetes model. Pharmacogn. Mag. 14, 167–173.

Donath, M.Y., Gross, D.J., Cerasi, E. and Kaiser, N. 1999. Hyperglycemia-induced beta-cell apoptosis in pancreatic islets of *Psammomys obesus* during development of diabetes. Diabetes 48, 738–744.

Ebaid, H., Habila, M., Hassan, I., Al-Tamimi, J., Omar, M.S., Rady, A. and Alhazza, I.M. 2021. Curcumin-containing silver nanoparticles prevent carbon tetrachloride- induced hepatotoxicity in mice. Comb. Chem. High Throughput. Screen. 24, 1609–1617.

Gadelmawla, M.H., Alazzouni, A.S., Farag, A.H., Gabri, M.S. and Hassan, B.N. 2022. Enhanced effects of ferulic acid against the harmful side effects of chemotherapy in colon cancer: docking and *in vivo* study. JoBAZ 83, 28.

Ganugula, R., Arora, M., Jaisamut, P., Wiwattanapatapee, R., Jorgensen, H.G., Venkatpurwar, V.P., Zhou, B., Rodrigues Hoffmann, A., Basu, R., Guo, S. and Majeti, N. 2017. Nano-curcumin safely prevents streptozotocin-induced inflammation and apoptosis in pancreatic beta cells for effective management of Type 1 diabetes mellitus. Br. J. Pharmacol. 174, 2074–2084.

Grama, C.N., Suryanarayana, P., Patil, M.A., Raghu, G., Balakrishna, N., Kumar, M.N. and Reddy, G.B. 2013. Efficacy of biodegradable curcumin nanoparticles in delaying cataract in diabetic rat model. PLoS One 8, e78217.

Greene, M.W. and Chen, T.T. 1999. Characterization of teleost insulin receptor family members. II. Developmental expression of insulin-like growth factor type I receptor messenger RNAs in rainbow trout. Gen. Comp. Endocrinol. 115, 270–281.

Han, X., Tao, Y.L., Deng, Y.P., Yu, J.W., Cai, J., Ren, G.F., Sun, Y.N. and Jiang, G.J. 2017. Metformin ameliorates insulitis in STZ-induced diabetic mice. Peer J. 5, e3155.

Hassan, I., Al-Tamimi, J., Ebaid, H., Habila, M.A., Alhazza, I.M. and Rady, A.M. 2023. Silver nanoparticles decorated with curcumin enhance the efficacy of metformin in diabetic rats via suppression of hepatotoxicity. Toxics 11(10), 867.

Hettiarachchi, S.S., Dunuweera, S.P., Dunuweera, A.N. and Rajapakse, R.M.G. 2021. Synthesis of curcumin nanoparticles from raw turmeric rhizome. ACS Omega 6, 8246–8252.

Huang, T.H., Peng, G., Kota, B.P., Li, G.Q., Yamahara, J., Roufogalis, B.D. and Li, Y. 2005. Anti-diabetic action of *Punica granatum* flower extract: activation of PPAR-gamma and identification of an active component. Toxicol. Appl. Pharmacol. 207, 160–169.

Ibrahim, R.M., Abdelhafez, H.M., El-Shamy, S.A.E., Eid, F.A. and Mashaal, A. 2023. Arabic gum ameliorates systemic modulation in Alloxan monohydrate-induced diabetic rats. Sci. Rep. 13, 5005.

Inoguchi, T., Sonta, T., Tsubouchi, H., Etoh, T., Kakimoto, M., Sonoda, N., Sato, N,. Sekiguchi, N., Kobayashi, K. and Sumimoto, H. 2003. Protein kinase C–dependent increase in reactive oxygen species (ROS) production in vascular tissues of diabetes: role of vascular NAD (P) H oxidase. J. Am. Soc. Nephrol. 14, S227–S232.

Jiang, W., Kim, B.Y., Rutka, J.T. and Chan, W.C. 2008. Nanoparticle-mediated cellular response is size-dependent. Nat. Nanotechnol. 3, 145–150.

Jose, P., Sundar, K., Anjali, C.H. and Ravindran, A. 2015. Metformin-loaded BSA nanoparticles in cancer therapy: a new perspective for an old antidiabetic drug. Cell Biochem. Biophys. 71, 627–36.

Kapoor, R., Srivastava, S. and Kakkar, P. 2009. Bacopa monnieri modulates antioxidant responses in brain and kidney of diabetic rats. Environ. Toxicol. Pharmacol. 27, 62–69.

Komolafe, O., Adeyemi, D., Adewole, S. and Obuotor, E. 2009. Streptozotocin-induced diabetes alters the serum lipid profiles of adult wistar rats. Int. J. cardiovasc. Res. 7(1), 1–7.

Levinthal, G.N. and Tavill, A.S. 1999. Liver disease and diabetes mellitus. Clin. Diabetes 17, 73–74.

Li, LY., Li, LQ. and Guo, CH. 2010. Evaluation of *in vitro* antioxidant and antibacterial activities of Laminaria japonica polysaccharides. J. Med. Plants Res 4, 2194–2198.

Lipinski, C.A., Lombardo, F., Dominy, B.W. and Feeney, P.J. 2001. Experimental and computational approaches to estimate solubility and permeability in drug discovery and development settings. Adv. Drug Deliv. Rev. 46, 3–26.

Lu, G., Teng, X., Zheng, Z., Zhang, R., Peng, L., Zheng, F., Liu, J., Huang, H. and Xiong, H. 2016. Overexpression of a glucokinase point mutant in the treatment of diabetes mellitus. Gene Ther. 23, 323–329.

Matschinsky, F.M. and Wilson, D.F. 2019. The central role of glucokinase in glucose homeostasis: a perspective 50 years after demonstrating the presence of the enzyme in islets of Langerhans. Front. Physiol. 10, 148.

Nna, V.U., Bakar, A.B.A., Ahmad, A. and Mohamed, M. 2020. Diabetes-induced testicular oxidative stress, inflammation, and caspase-dependent apoptosis: the protective role of metformin. Arch. Physiol. Biochem. 126, 377–388.

Peiro, C., Lorenzo, O., Carraro, R. and Sanchez-Ferrer, C.F. 2017. IL-1beta inhibition in cardiovascular complications associated to diabetes mellitus. Front. Pharmacol. 8, 363.

Prasad, K., Mantha, S.V., Muir, A.D. and Westcott, N.D. 2000. Protective effect of secoisolariciresinol diglucoside against streptozotocin-induced diabetes and its mechanism. Mol. Cell Biochem. 206, 141–149.

Prasath, G.S. and Subramanian, S.P. 2013. Fisetin, a tetra hydroxy flavone recuperates antioxidant status and protects hepatocellular ultrastructure from hyperglycemia mediated oxidative stress in streptozotocin induced experimental diabetes in rats. Food Chem. Toxicol. 59, 249–255.

Robertson, R.P., Harmon, J., Tran, P.O. and Poitout, V. 2004. Beta-cell glucose toxicity, lipotoxicity, and chronic oxidative stress in type 2 diabetes. Diabetes 53(Suppl 1), S119–S124.

Roxo, D.F., Arcaro, C.A., Gutierres, V.O., Costa, M.C., Oliveira, J.O., Lima, T.F.O., Assis, R.P., Brunetti, I.L. and Baviera, A.M. 2019. Curcumin combined with metformin decreases glycemia and dyslipidemia, and increases paraoxonase activity in diabetic rats. Diabetol. Metab. Syndr. 11, 33.

Sanchez, S.S., Abregu, A.V., Aybar, M.J. and Sanchez Riera, A.N. 2000. Changes in liver gangliosides in streptozotocin-induced diabetic rats. Cell Biol. Int. 24, 897–904.

Seedevi, P., Ramu Ganesan, A., Moovendhan, M., Mohan, K., Sivasankar, P., Loganathan, S., Vairamani, S. and Shanmugam, A. 2020. Anti-diabetic activity of crude polysaccharide and rhamnose-enriched polysaccharide from G. lithophila on Streptozotocin (STZ)-induced in Wistar rats. Sci. Rep. 10, 556.

Shome, S., Talukdar, A.D., Choudhury, M.D., Bhattacharya, M.K. and Upadhyaya, H. 2016. Curcumin as potential therapeutic natural product: a nanobiotechnological perspective. J. Pharm. Pharmacol. 68, 1481–1500.

Sultan H.A, Ashry M, M H El-Bitar A, N Yassen N, E Abdelsalam M, A Moustafa M (2021) Synthetic Zeolite Supplementation as a Potential Candidate for the Therapy of Diabetic Syndrome. Pak J Biol Sci 24 (10):1067–1076. doi:10.3923/pjbs.2021.1067.1076

Steel, R.G. and Torrie, J.H. 1981. Principles and procedures of statistics, a biometrical approach. 2nd edition, New York, NY: McGraw-Hill Book Company.

Tahara, A., Matsuyama-Yokono, A., Nakano, R., Someya, Y. and Shibasaki, M. 2008. Hypoglycaemic effects of antidiabetic drugs in streptozotocin-nicotinamide-induced mildly diabetic and streptozotocin-induced severely diabetic rats. Basic Clin. Pharmacol. Toxicol. 103, 560–568.

Thota, R.N., Dias, C.B., Abbott, K.A., Acharya, S.H. and Garg, M.L. 2018. Curcumin alleviates postprandial glycaemic response in healthy subjects: a cross-over, randomized controlled study. Sci. Rep. 8, 13679.

Tiedge, M., Lortz, S., Munday, R. and Lenzen, S. 1999. Protection against the co-operative toxicity of nitric oxide and oxygen free radicals by overexpression of antioxidant enzymes in bioengineered insulin-producing RINm5F cells. Diabetologia 42, 849–855.

Tolman, K.G., Fonseca, V., Dalpiaz, A. and Tan, M.H. 2007. Spectrum of liver disease in type 2 diabetes and management of patients with diabetes and liver disease. Diabetes Care 30, 734–743.

Wanninger, S., Lorenz, V., Subhan, A. and Edelmann, F.T. 2015. Metal complexes of curcumin--synthetic strategies, structures and medicinal applications. Chem. Soc. Rev. 44, 4986–5002.

Wojcik, M., Krawczyk, M., Wojcik, P., Cypryk, K. and Wozniak, L.A. 2018. Molecular mechanisms underlying curcumin-mediated therapeutic effects in type 2 diabetes and cancer. Oxid. Med. Cell Longev. 2018, 9698258.

Yachamaneni, J. and Dhanraj, S. 2017. Anti-hepatotoxic and antioxidant activity of Limnanthemum indicum against carbon tetrachloride induced liver toxicity in rats. Indian J. Pharm. Educ. Res. 51, 321–328.

Zhang, T., Guo, P., Zhang, Y., Xiong, H., Yu, X., Xu, S., Wang, X., He, D. and Jin, X. 2013. The antidiabetic drug metformin inhibits the proliferation of bladder cancer cells *in vitro* and *in vivo*. Int. J. Mol. Sci. 14, 24603–24618.